Electronic Supplementary Material (ESI) for Polymer Chemistry.

Supramolecular polymer network gels constructed by a pillararene-containing polymer and their applications in adhesion between semihard materials

Yujie Cheng,[ab] Xiaoqing Lv,[a] Bicong Liang,[c] Xuehong Wei[a], Pi Wang*[c] and Danyu Xia*[a]*

[a] *Scientific Instrument Center, Shanxi University, Taiyuan 030006, P. R. China.*

[b] *School of Chemistry and Chemical Engineering, Shanxi University, Taiyuan 030006, P. R. China.*

[c] *College of Materials Science and Engineering, Taiyuan University of Technology, Taiyuan 030024, P.R. China.*

Electronic Supplementary Information

[Note] The movie files of the macroscopic adhesive between semihard materials are uploaded in Supporting Information.

*Movie S1. Macroscopic self-assembly between.two pieces of **HGCG** semihard materials in a petri dish, adding of 2 μL of chloroform, which stick firmly together.*

*Movie S2. Macroscopic self-assembly between two pieces of **MCCG** semihard materials in a petri dish, adding of 2 μL of chloroform, which stick firmly together.*

*Movie S3. Microscopic images of the adhesive surfaces of two pieces of **HGCG** semihard materials.*

*Movie S4. Microscopic images of the adhesive surfaces of two pieces of **MCCG** semihard materials.*

1. Materials and methods

All reagents were commercially available and used as supplied without further purification. Compounds **H**,[S1] **G2**,[S2] **1**,[S3] **2** [S4] and **3**[S5]were prepared according to published procedures. Both ^{1}H NMR and ^{13}C NMR spectra were recorded with a Bruker Avance DMX 600 spectrophotometer. Scanning Electron Microscopy (SEM) investigations were carried out on a TASCAN (LYRA3) instrument. Gel permeation chromatography (GPC) analysis was carried out with a Anton Paar MCR 102 GPC analysis system, using THF as the eluent, flow rate of 1 mL/min. Linear PS standards were applied as calibration samples. X-ray diffraction (XRD) measurements were carried out on a Bruker D2 PHASER. Rheological properties were tested on a Modular Compact Rheometer-MCR 102 instrument with a 25 mm measuring plate PP25. All rheological experiments unless otherwise specified were carried out at 298 K. Not use of a solvent trap in this rheometry experiments. The strain used for the frequency sweeps is 0.2%. Adhesion interfaces were measured using a digital inverted microscope (SMZ-168 SERIES, Advanced Microscopy Group). FT-IR spectra were recorded on a Thermo Scientific Nicolet iS50 spectrometer. The equipment of the UV irradiation is LE-SP Series Light Source Controller and LE-SP Series Stabilized Light source. The mechanical properties of the xerogels were measured using a rupture testing system (Computer Controlled Electromechanical Universal Testing Machine, ETM, 304C).

Gel preparation: The gel **HGCG** was obtained by mixing the chloroform solutions of **P** (100 mg) and TFA (7.00 μL) after ultrasounding for 0.5 hours and then waiting for the solvent to evaporate slowly at 25 ℃. Similarly, the gel **MCCG** was obtained by mixing the chloroform solutions of **P** (100 mg) and Cu(II) (6.00 mg) after ultrasounding for 0.5 hours. After filtering the redundant copper ion, the solution was waited for the solvent to evaporate slowly at 25 ℃.

SEM sample preparation: 10 mg of **P** was dissolved in 0.279 mL of chloroform solution, and then ultrasounded for 0.5 hours. After standing overnight, the solution was dropped on silicon wafer. After drying, the SEM sample of **P** was prepared by gold-coating. 0.700 μL of TFA was added to 10.0 mg of **P** in chloroform and then ultrasounded for 0.5 hours. After standing overnight. The solution was dropped on silicon wafer. After drying, the SEM sample of **HGCG** was prepared by gold-coating. Similarly, 0.6 mg of Cu(II) was added to 10.0 mg of **P** in chloroform, and then ultrasounded for 0.5 hours. After standing overnight, the redundant copper ion was filtered and the solution was dropped on silicon wafer. After drying, the SEM sample of **MGCG** was prepared by

gold-coating. The solution of **P**, **HGCG** and **MCCG** after irradiation with UV light at 365 nm for 2 hours in chloroform. The solutions were dropped on silicon wafer, respectively. After drying, the SEM samples of **P**, **HGCG** and **MCCG** after irradiation with UV light were prepared by gold-coating.

Tensile tests sample preparation: The xerogel **HGCG** (8.15 × 4.50 × 3.10 mm^3) piece was prepared as the gel **HGCG** for 2 days. Similarly, the xerogel **MCCG** (7.75 × 5.00 × 3.50 mm^3) pieces was obtained as the gel **MCCG** xerogel(x) for 2 days.

*2. Synthesis of compounds **G2**, **1**, **2**, **3** and polymer **P***

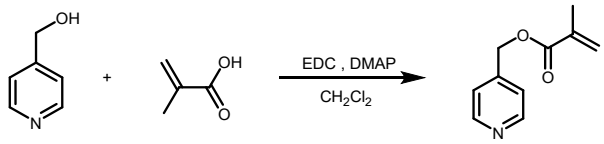

Scheme S1 Synthesis of **G2**.

Synthesis of **G2**: Methacrylic acid (0.860 g, 10.0 mmol), 4-pyridinemethanol (1.00 g, 9.16 mmol) and 4-dimethylaminopyridine (DMAP) (14.0 mg, 0.110 mmol) was dissolved in 100 mL of dichloromethane (DCM) at 0 ℃. Then DCM solution of 1-(3-Dimethylaminopropyl)-3-ethylcarbodiimide hydrochloride (EDC) (2.07 g, 11.0 mmol) was slowly added at 0 ℃. The reaction mixture was stirred at 25 ℃ for 24 hours and then filtered. The filtrate was washed thoroughly with saturated $NaHCO_3$ and then the organic phase was dried with anhydrous Na_2SO_4 and filtered. DCM was removed via rotary evaporation and the residue was purified by chromatography on silica gel methanol/ethyl acetate, (*v*/*v* = 1:1) to give **G2** as a yellow viscous oil (0.580 g, 72.0%). The ^1H NMR spectrum of **G2** is shown in Fig. S1. ^1H NMR (600 MHz, $CDCl_3$, 298 K) δ (ppm): 8.62–8.61 (d, 2H), 7.29–7.28 (d, 2H), 6.22(s, 1H), 5.66 (s, 1H), 5.21 (s, 2H), 2.00 (s, 3H). The ^{13}C NMR spectrum of **G2** is shown in Fig. S2. ^{13}C NMR (150 MHz, $CDCl_3$, 298 K) δ (ppm): 166.97, 149.99, 145.47, 135.91, 126.68, 121.95, 64.52, 18.46.

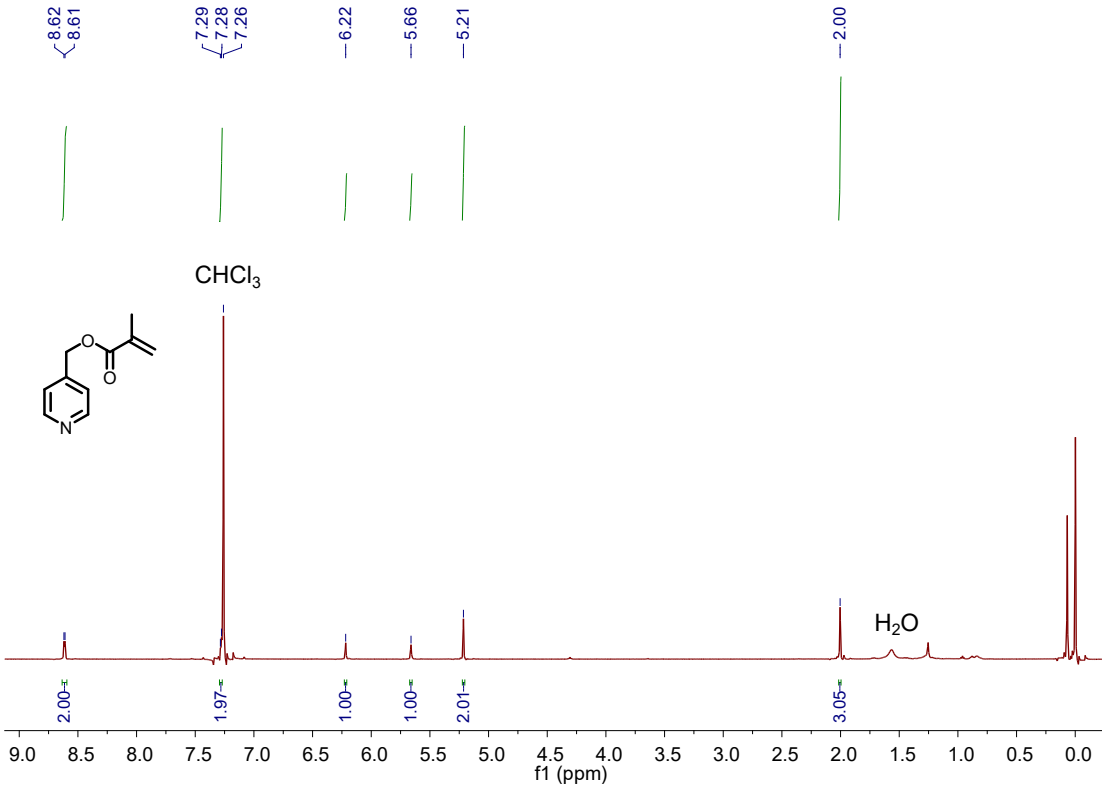

Fig. S1 ^{1}H NMR spectrum (600 MHz, $CDCl_3$, 298 K) of **G2**.

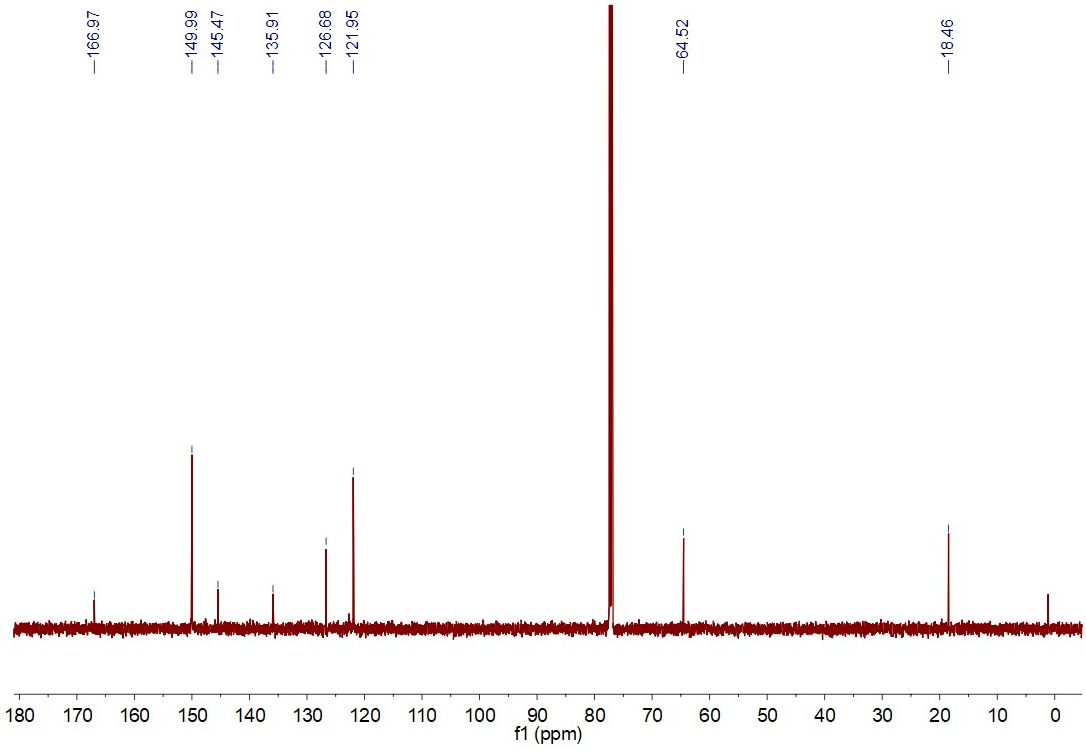

Fig. S2 ^{13}C NMR spectrum (150 MHz, $CDCl_3$, 298 K) of compound **G2**.

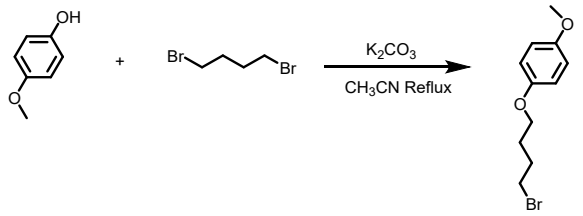

Scheme S2 Synthesis of **1**

Synthesis of **1**: Under a nitrogen atmosphere, 4-methoxyphenol (5.00 g, 40.2 mmol) and 1,4-dibromobutane (17.4 g, 80.5 mmol) were dissolved in acetonitrile (300 mL), followed by addition of K_2CO_3 (16.7 g, 121 mmol). The mixture was stirred and refluxed at 85 °C for 24 hours. Then the cooled reaction mixture was filtered and washed with dichloromethane. The filtrate was concentrated and the residue was purified by column chromatography (eluent: petroleum ether/dichloromethane = 5:1, *v*/*v*) to afford the desired product **1** as a white solid (8.45 g, 81.0%). The ^{1}H NMR spectrum of **1** is shown in Fig. S3. ^{1}H NMR ($CDCl_3$, 600 MHz, 298 K) δ (ppm): 6.83 (s, 4H), 3.96–3.94 (t, J = 7.5 Hz, 2H), 3.77 (s, 3H), 3.50–3.48 (t, J = 7.5 Hz, 2H), 2.09–2.04 (m, 2H), 1.94–1.91 (m, 2H).

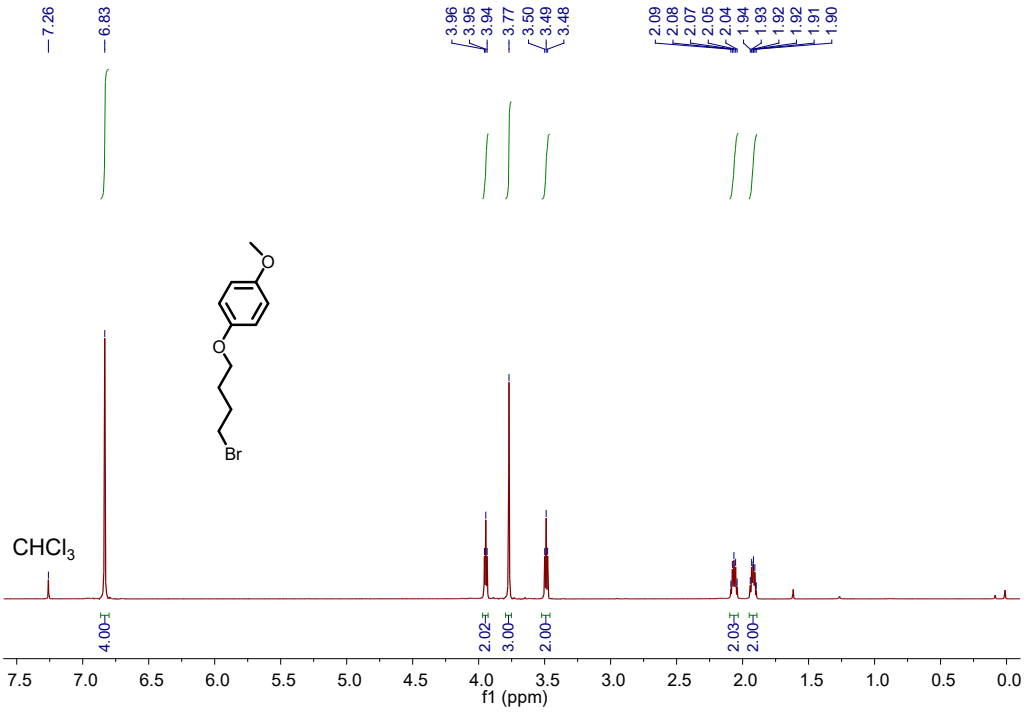

Fig. S3 ^{1}H NMR spectrum (600 MHz, $CDCl_3$, 298 K) of **1**.

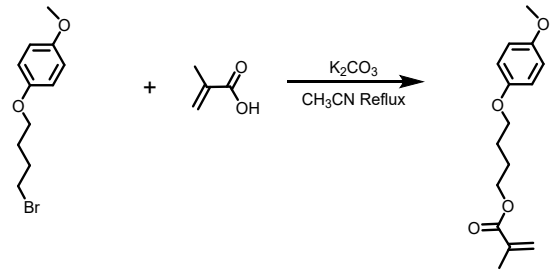

Scheme S3 Synthesis of **2**

Synthesis of **2**: Firstly, compound **1** (4.00 g, 15.4 mmol) and methacrylic acid (2.65 g, 30.8 mmol) were added in dry acetonitrile (200 mL) under stirring at 25 ℃ for 0.5 hours, then potassium carbonate (4.26 g, 30.8 mmol) was added. The mixture was stirred and refluxed at 85°C for 24 hours under nitrogen atmosphere. After the reaction was completed, the resulting mixture was filtered and the residue was washed with dichloromethane. Evaporation of the solvent under reduced pressure and further purification was carried out by column chromatography using dichloromethane/petroleum ether (*v*/*v* = 1:2) as eluent to afford 2.88 g of product as to give **2** as a transparent oil. Yield: 70.6%. The ^{1}H NMR spectrum of **2** is shown in Fig. S4. ^{1}H NMR ($CDCl_3$, 600 MHz, 298 K) δ (ppm): 6.83 (s, 4H), 6.10 (s, 1H), 5.55(s, 1H), 4.22 (s, *J* = 12 Hz, 2H), 3.95 (s, *J* = 12 Hz, 2H), 3.77 (s, 3H), 1.95 (s, 3H), 1.87 (s, 4H). The ^{13}C NMR spectrum of **2** is shown in Fig. S5. ^{13}C NMR (150 MHz, $CDCl_3$, 298 K) δ (ppm): 167.62, 153.94, 153.21, 136.56, 125.49, 115.56, 114.79, 68.07, 64.51, 55.88, 26.18, 25.58, 18.47.

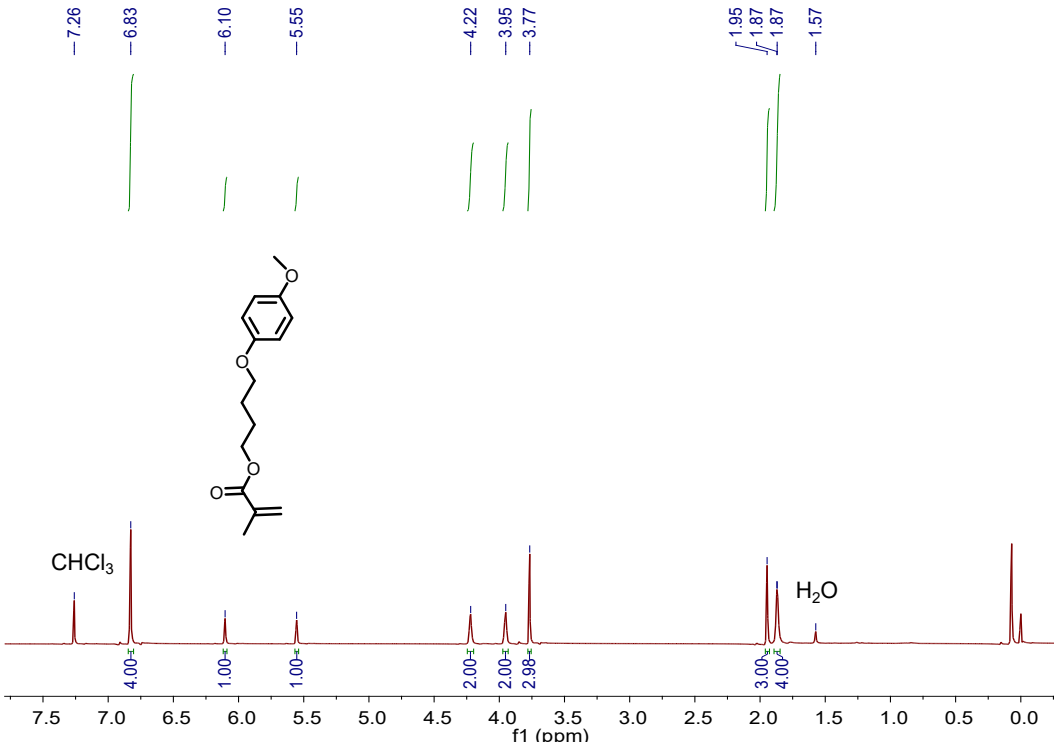

Fig. S4 ^{1}H NMR spectrum (600 MHz, $CDCl_3$, 298 K) of **2**.

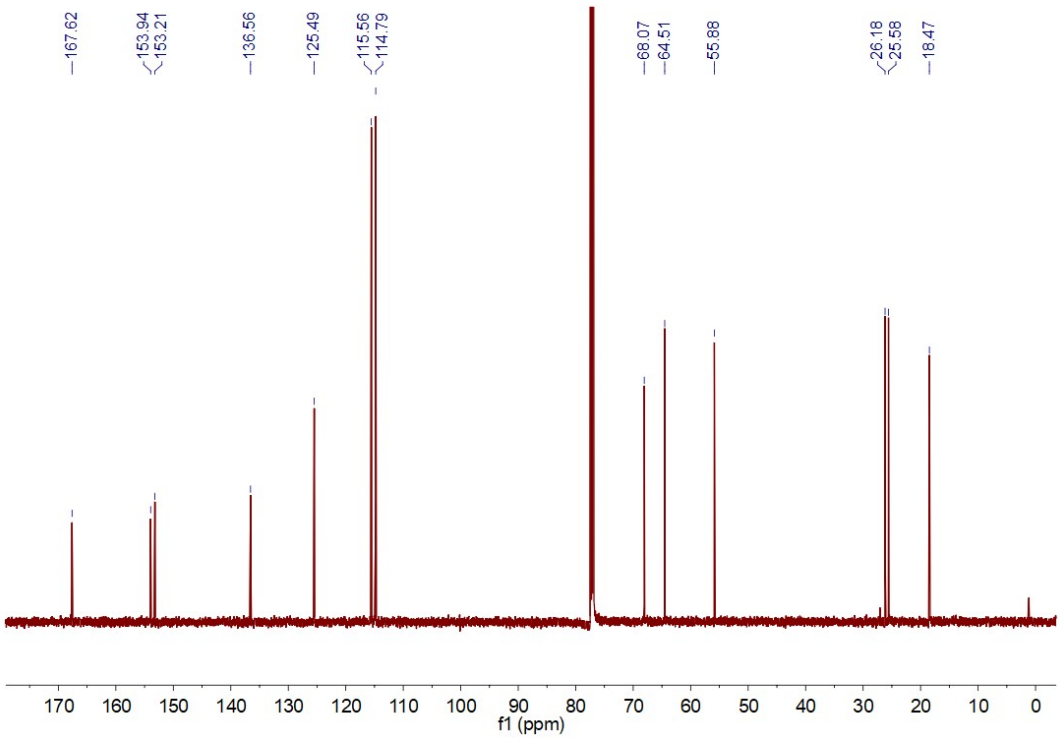

Fig. S5 ^{13}C NMR spectrum (150 MHz, $CDCl_3$, 298 K) of compound **2**.

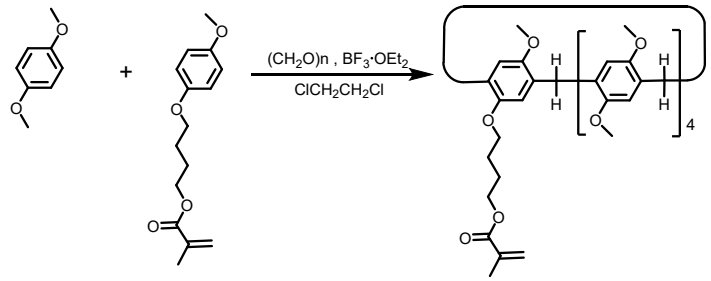

Scheme S4 Synthesis of **3**

Synthesis of **3**: Boron trifluoride etherate [(BF_3•OEt_2), 5.00 mL, 39.6 mmol] was added to a CH_2ClCH_2Cl (300 mL), solution with compound **2** (3.60 g, 13.6 mmol), 1,4-dimethoxybenzene (7.53 g, 54.5 mmol) and paraformaldehyde (4.08 g, 136 mmol). The solution was stirred at 25 °C for 20 minutes, washed with water and dried with Na_2SO_4. CH_2ClCH_2Cl was removed under vacuum and the residue was purified by column chromatography on silica gel with mixture of petroleum ether and CH_2Cl_2 (1:2, *v*/*v*) as the eluent to afford methyl methacrylate functionalized pillar[5]arene **3** (2.50 g), white solid, yield: 21.0%. The ^{1}H NMR spectrum of **3** is shown in Fig. S6. ^{1}H NMR (600 MHz, $CDCl_3$, 298 K) δ (ppm): 6.77–6.71(m, 10H), 6.11 (s, 1H), 5.57 (s, 1H), 4.24–4.22(t, 2H), 3.88–3.86 (t, 2H,), 3.79–3.76 (q, 10H), 3.65–3.62 (m, 27H), 2.06–1.86 (m, 7H). The ^{13}C NMR spectrum of **3** is shown in Fig. S7. ^{13}C NMR (150 MHz, $CDCl_3$, 298 K) δ (ppm): 167.60, 150.96, 150.93, 150.90, 150.89, 150.86, 150.00, 136.55, 128.42, 128.36, 128.35, 125.53, 115.05, 114.28, 114.25, 114.21, 114.16, 114.14, 114.11, 114.06, 68.01, 64.57, 55.97, 55.92, 55.88, 55.82, 53.21, 29.90, 29.84, 29.76, 29.72, 29.54, 26.61, 25.85.

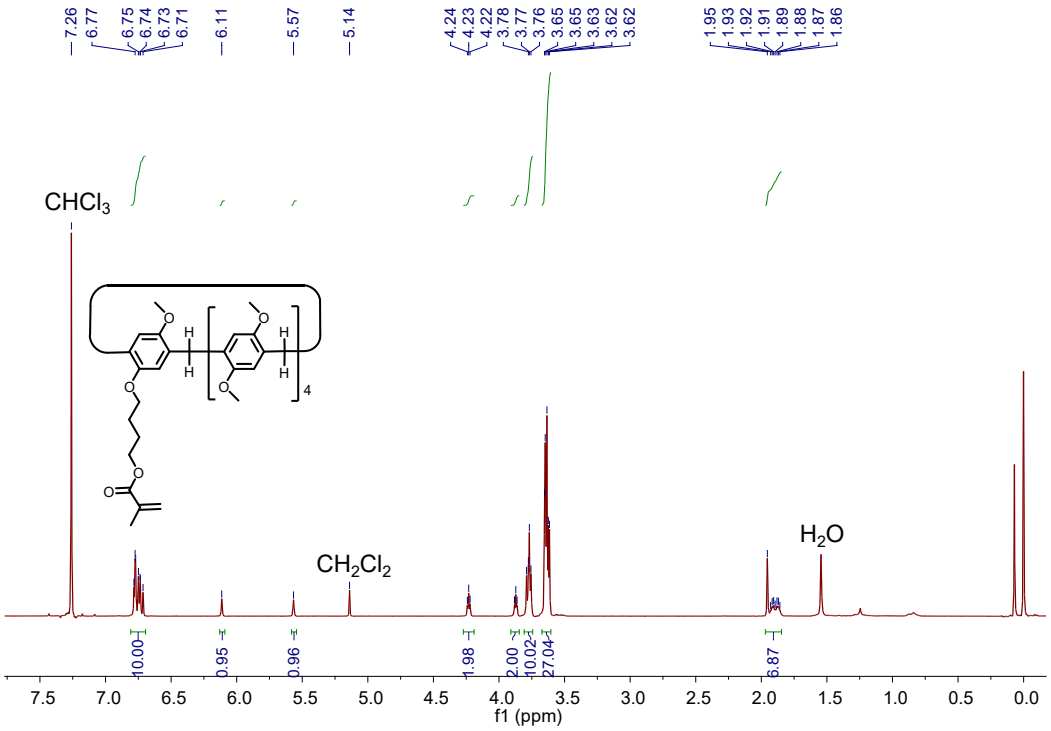

Fig. S6 ^{1}H NMR spectrum (600 MHz, $CDCl_3$, 298 K) of **3**.

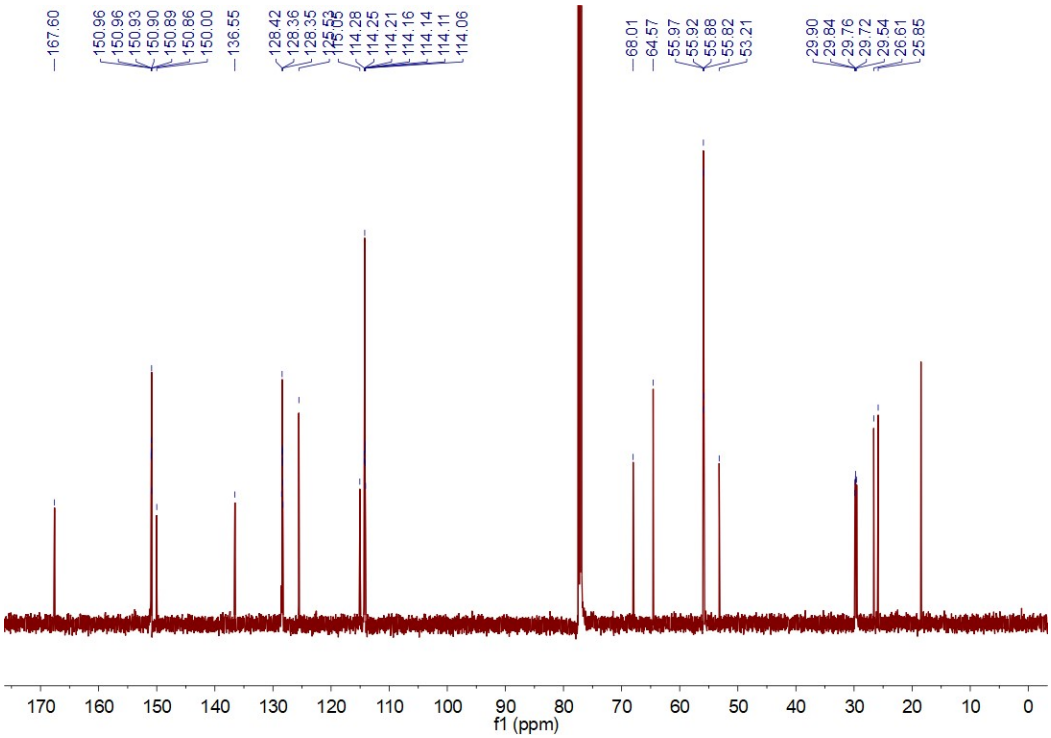

Fig. S7 ^{13}C NMR spectrum (150 MHz, $CDCl_3$, 298 K) of compound **3**.

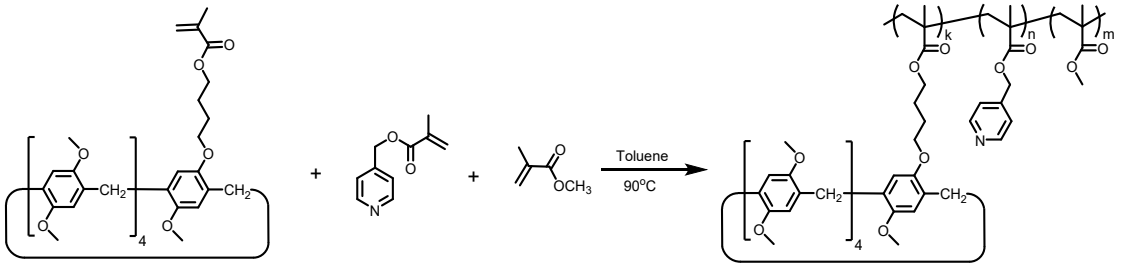

Scheme S5 Synthesis of polymer **P**

Synthesis of polymer **P**: A mixture of compound **G2** (2.51 g, 2.50 mmol), compound **3** (0.425 g, 2.50 mmol), methyl methacrylate (2.50 g, 25.0 mmol) and azobisisobutyronitrile (AIBN) (4.00 mg, 0.0280 mmol) in 10 mL of toluene was stirred at25 ℃. The solution was degassed by three freeze-pump-thaw cycles and then heated at 90 ºC for 6 hours. The polymerization was stopped through cooling with an ice bath. The reaction mixture was diluted with $CHCl_3$ (10 mL), precipitated in ethanol (400 mL) thrice, and dried under vacuo to afford the polymer **P** as a white solid (2.50 g, 46.0%), which was characterized by ^{1}H NMR (Fig. S8) and GPC (Fig. S9). The value of *k*/*n*/*m* is 31.02/31.02/232.06, calculated by the integration area of proton H_1 owing to pillar[5]arene aromatic ring, area of proton H_{10} belonging to 4-pyridinemethoxy ester group and area of proton H_{11} attributed to the methoxy group of methyl methacrylate moieties. The molecular weight determined by GPC was 55 kDa with polydispersity of 1.75.

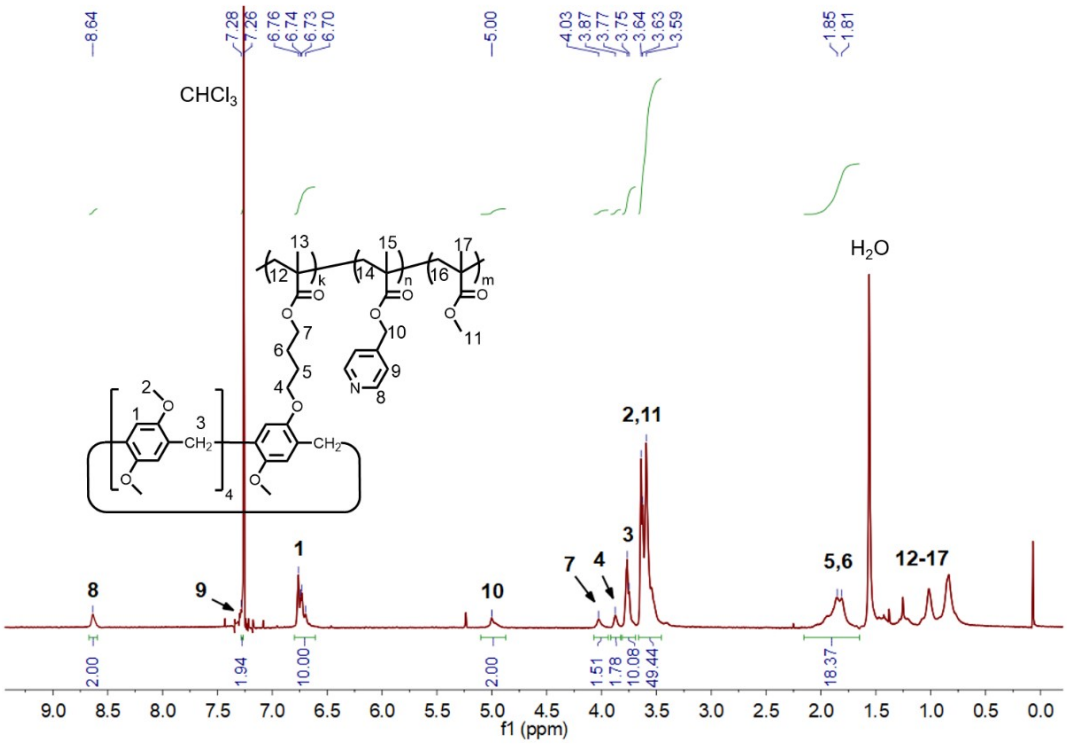

Fig. S8 ^{1}H NMR spectrum (600 MHz, $CDCl_3$, 298 K) of **P**.

*3. GPC result of polymer **P***

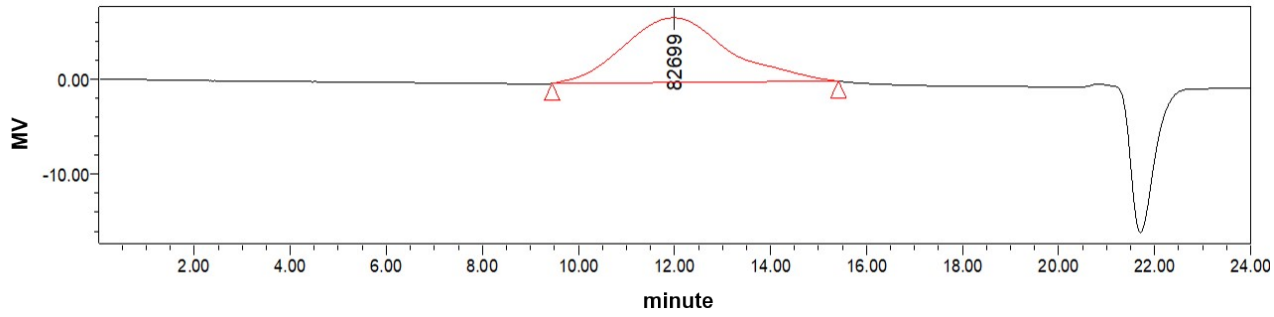

Fig. S9 GPC result of polymer **P** in THF.

Table S1 GPC analysis of polymer **P** using conventional calculations, with polystyrene as the standard and THF as the solvent.

***M*n**	***M*w**	***Mp***	***Mz***	**PDI**
55611.10	97432.15	82699.09	151540.6	1.752027

According to *M*n and the ratio of *k*/*n*/*m*, it can be calculated that the values of *k*, *n*, and *m* were 31.02, 31.02 and 232.06, respectively.

*4. [1]H NMR experiments on the **H** and **G2***

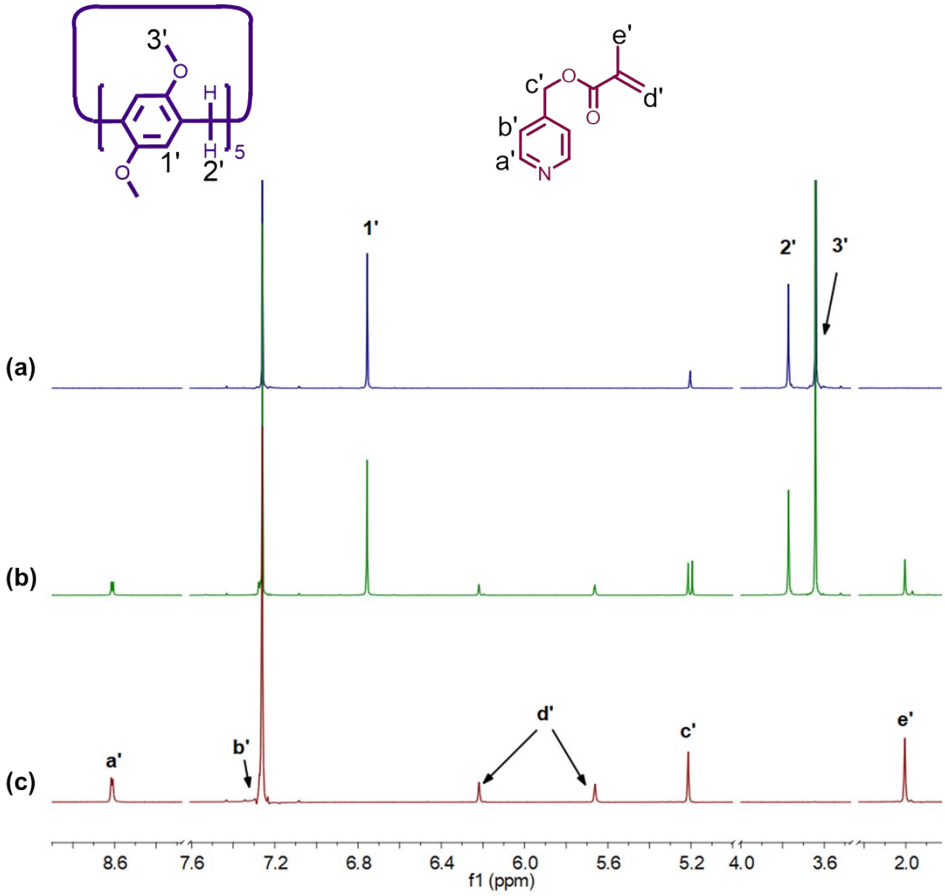

Fig. S10 Partial [1]H NMR spectra (600 MHz, $CDCl_3$, 298 K): (a) **H** (5.00 mM); (b) **H** (5.00 mM) and **G2** (5.00 mM); (c) **G2** (5.00 mM).

*5. [1]H NMR experiments on the **H** and **G1***

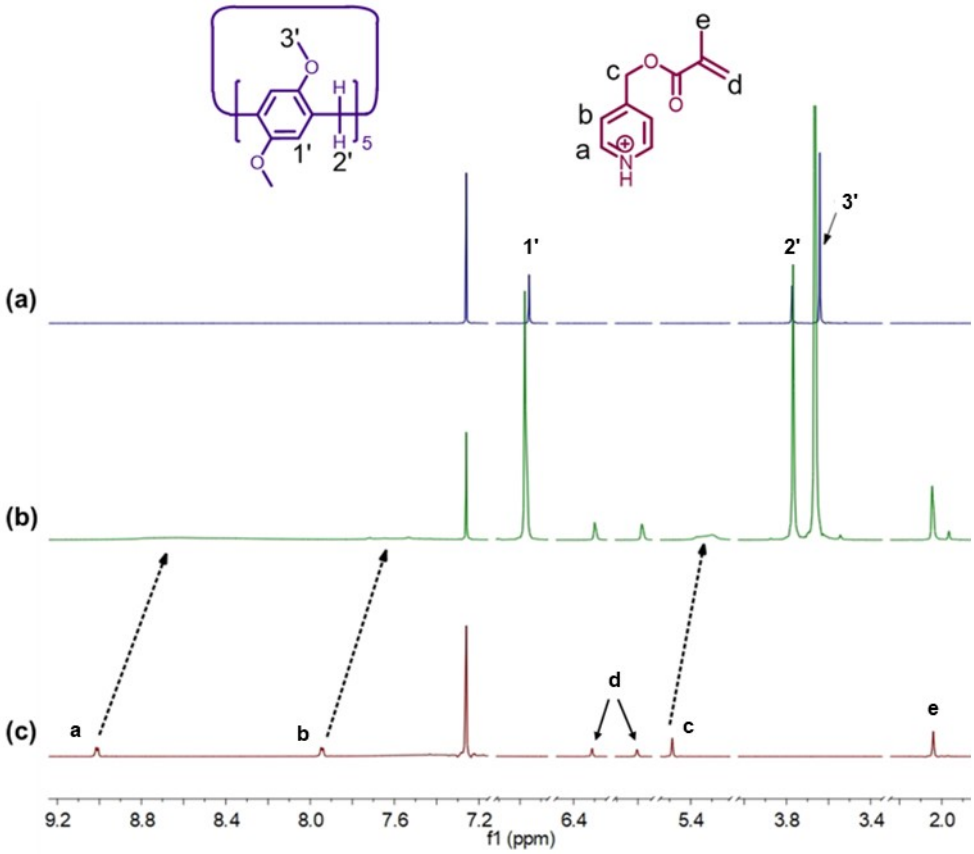

Fig. S11 Partial [1]H NMR spectra (600 MHz, $CDCl_3$, 298 K): (a) **H** (5.00 mM); (b) **H** (5.00 mM) and **G1** (5.00 mM); (c) **G1** (5.00 mM).

*6. Complexation study on **H** and **G1***

To determine the stoichiometry and association constant between **H** and **G1**, ^{1}H NMR titration was done with solutions which had a constant concentration of **G1** (1.00 mM) and different concentrations of **H**. By a non-linear curve-fitting method, the association constant between the **H** and **G1** was calculated. By a mole ratio plot, a 1:1 stoichiometry was obtained for this system.

The non-linear curve-fitting was based on the equation:

$$\Delta\delta = (\Delta\delta_\infty/[\mathbf{G1}]_0)\ (0.5[\mathbf{H}]_0 + 0.5([\mathbf{G1}]_0 + 1/K_a) - (0.5([\mathbf{H}]_0^2 + (2[\mathbf{H}]_0(1/K_a - [\mathbf{G1}]_0)) + (1/K_a + [\mathbf{G1}]_0)^2)^{0.5})) \quad \text{(Eq.1)}$$

Where in $\Delta\delta$ is the chemical shift change of H_a on **G1** at $[\mathbf{H}]_0$, Δ_∞ is the chemical shift change of H_a when the **G1** is completely complexed, $[\mathbf{G1}]_0$ is the fixed initial concentration of the **G1**, and $[\mathbf{H}]_0$ is the varying concentration of $\mathbf{H}^{S6}$.

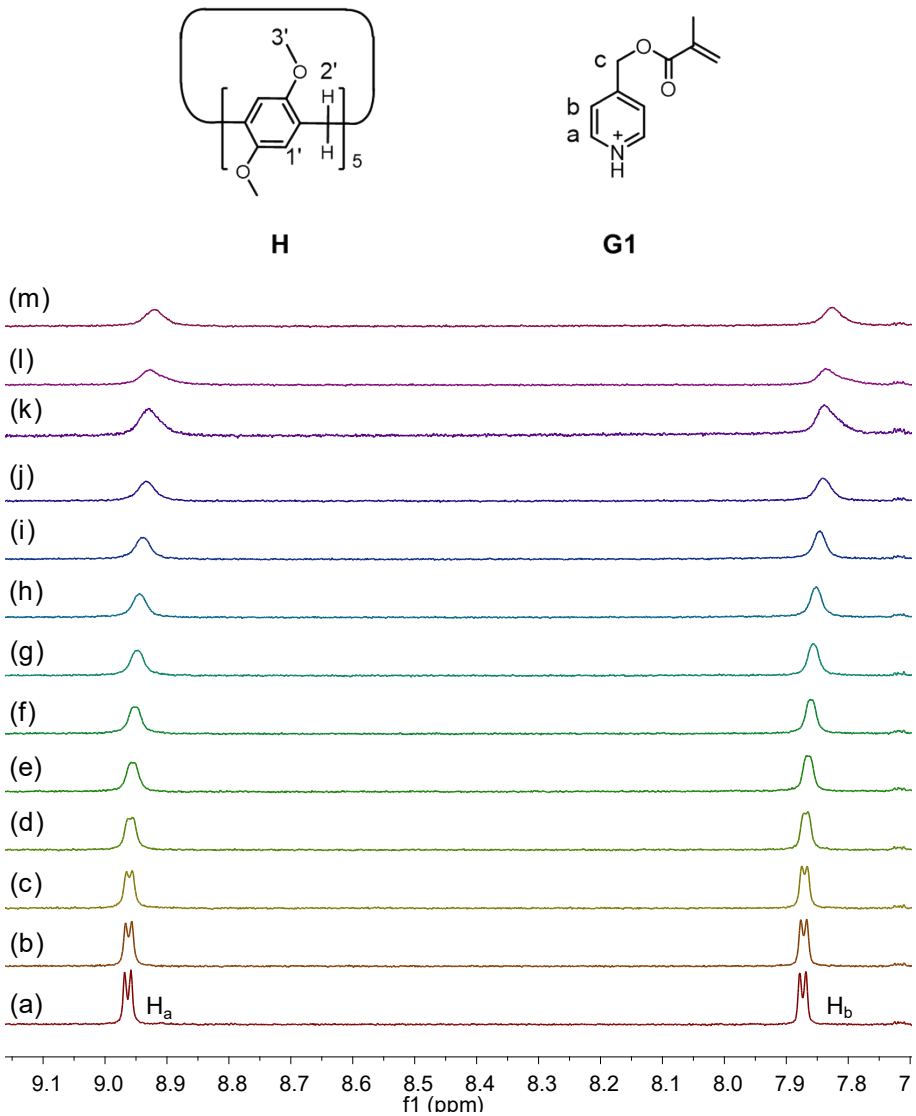

Fig. S12 Partial ^{1}H NMR spectra (600 MHz, $CDCl_3$, 298 K) of **G1** at a concentration of 1.00 mM with different concentrations of **H**: (a) 0 mM; (b) 0.10 mM; (c) 0.19 mM; (d) 0.38 mM; (e) 0.56 mM; (f) 0.82 mM; (g) 1.07 mM; (h) 1.38 mM; (i) 1.66 mM; (j) 2.30 mM; (k) 3.33 mM; (l) 4.11 mM; (m) 5.23 mM.

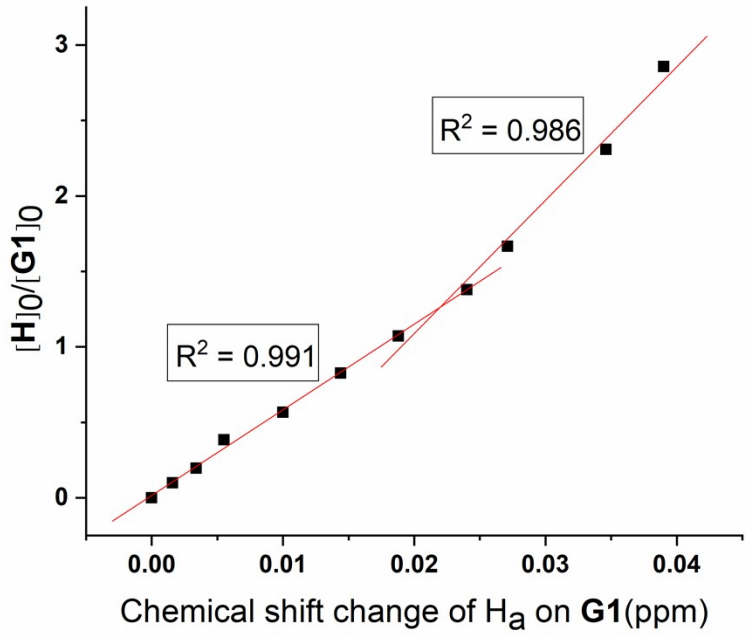

Fig. S13 Mole ratio plot for the complexation between **H** and **G1**, indicating a 1:1 stoichiometry.

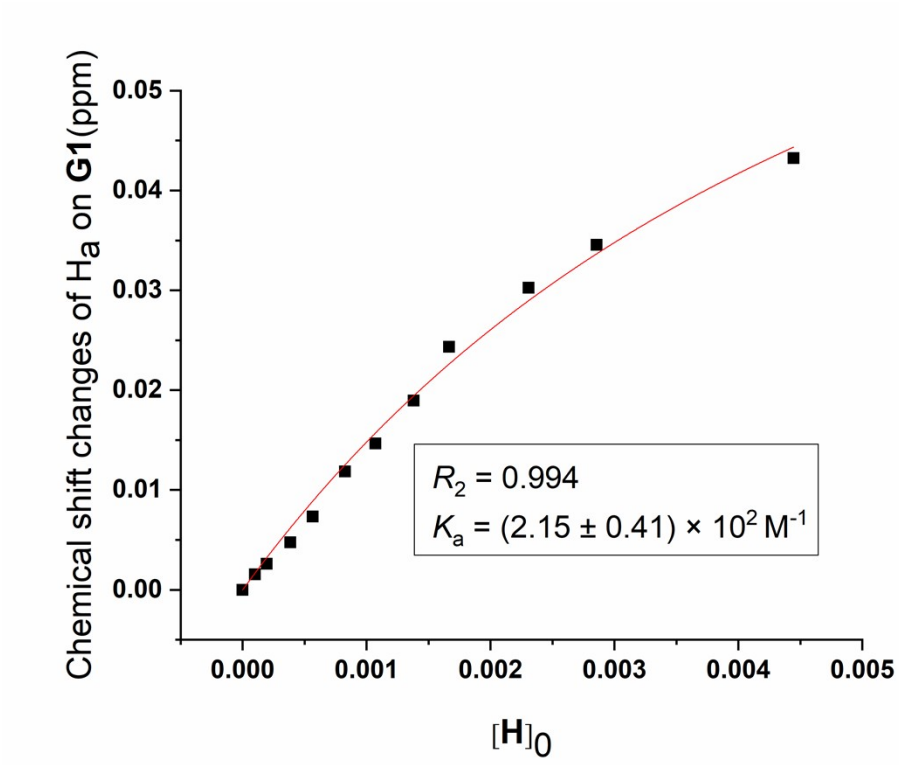

Fig. S14 The chemical shift changes of H_a on **G1** upon addition of **H**. The black solid line was obtained from the non-linear curve-fitting using Eq.1.

*7. Rheological tests of **HGCG** and **MCCG***

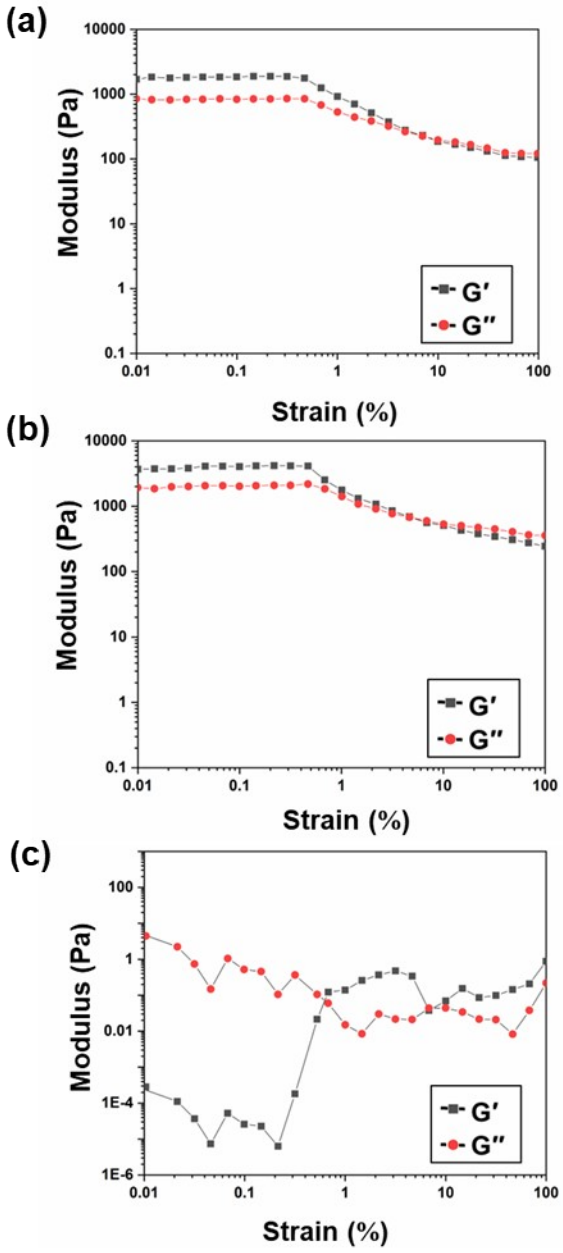

Fig. S15 Storage modulus (G′) and loss modulus (G″) as a function of strain (10 rad/s): (a) The gel **HGCG** (20.0 mM) (10 rad/s), (b) The gel **MCCG** (20.0 mM) (10 rad/s) and (c) **P** (20.0 mM).

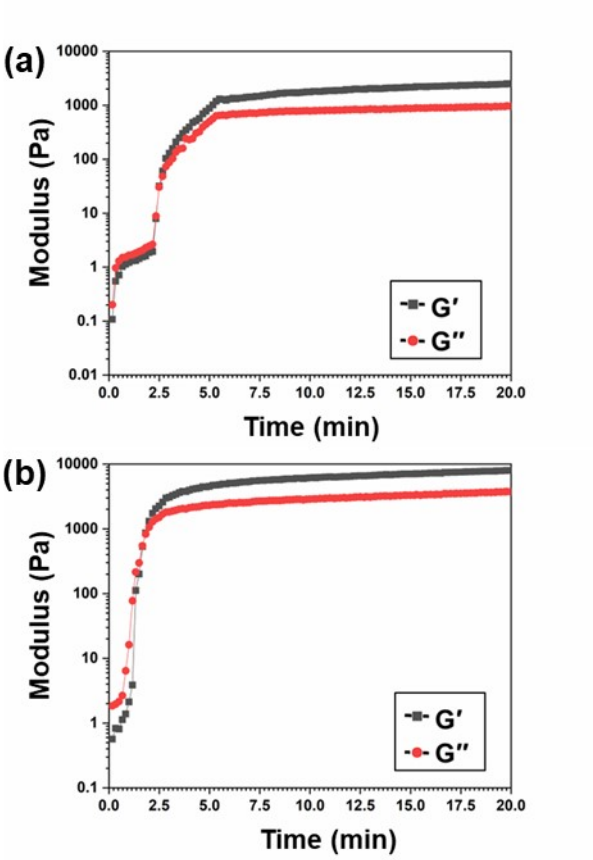

Fig. S16 Storage modulus (G′) and loss modulus (G″) as a function of time (0.2% strain, 10 rad/s): (a) The gel **HGCG** and (b) The gel **MCCG** examined by rheological tests.

*8. The stimuli-responsive characters of **HGCG** and **MCCG***

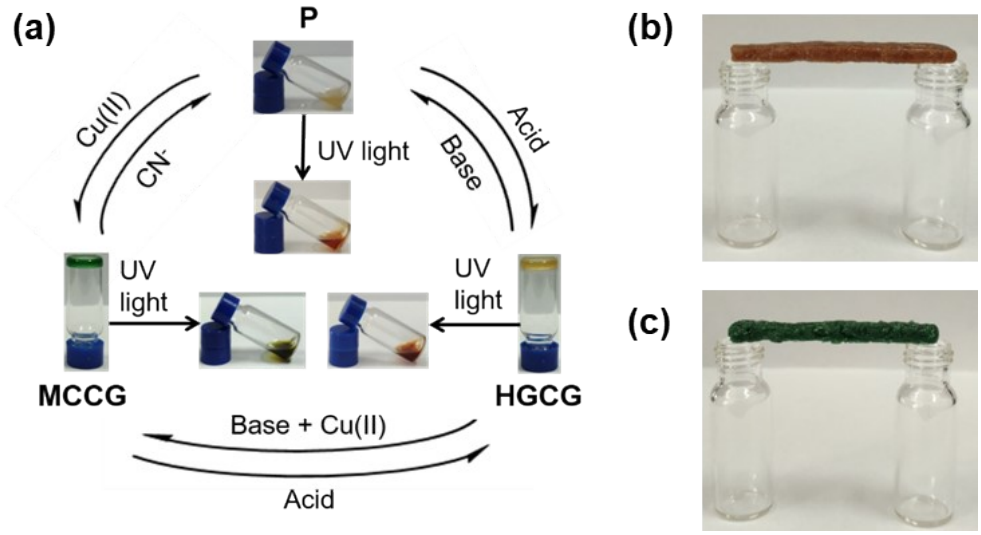

Fig. S17 (a) The reversible gel–sol transitions of the supramolecular gels triggered by a variety of stimuli. (b) A bridge constructed by the gel **HGCG**. (c) A bridge constructed by the gel **MCCG**.

*9. [1]H NMR experiments of the pH-responsiveness of **HGCG***

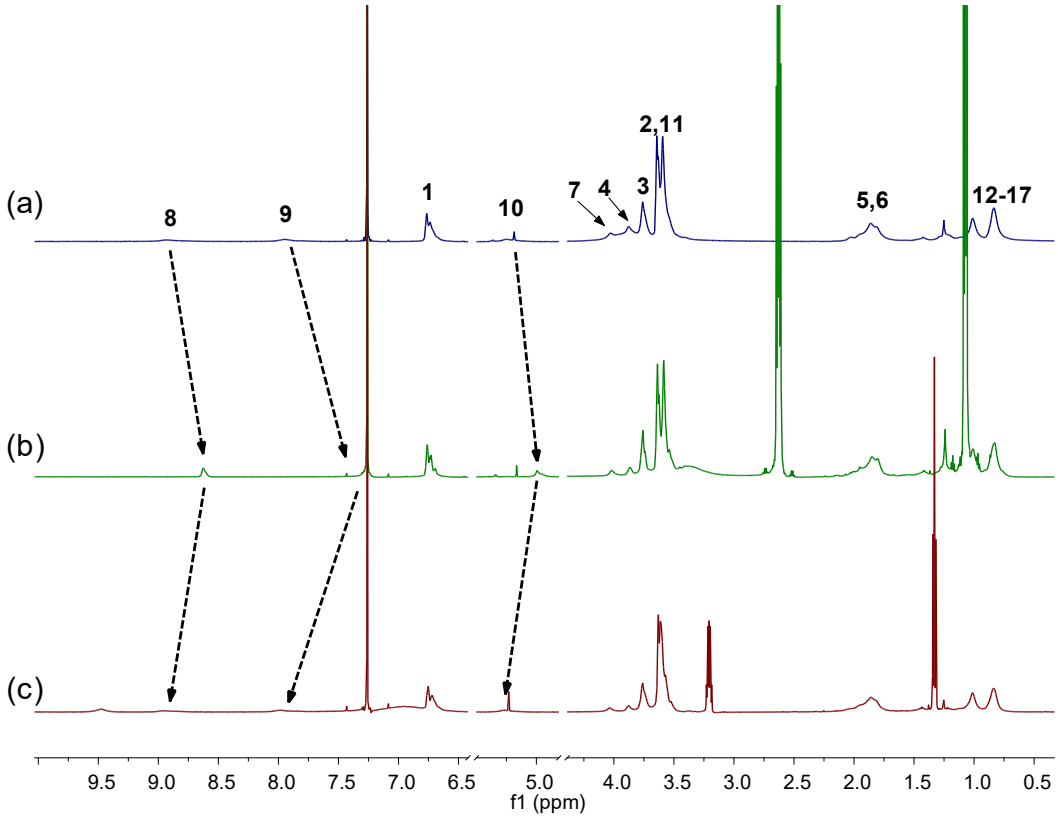

Fig. S18 Partial [1]H NMR spectra (600 MHz, $CDCl_3$, 298 K): (a) The gel **HGCG** (5.00 mM); (b) After addition of 1.00 equimolar TEA to sample a; (c) After further addition of 1.50 equimolar TFA to sample b.

*10. XRD experiments of the pH-responsiveness of **HGCG***

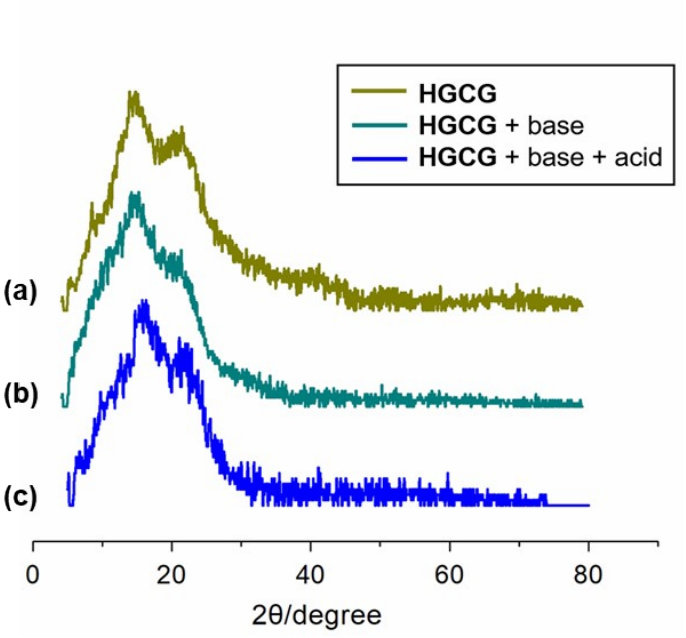

Fig. S19 XRD analysis: (a) **HGCG**; (b) after addition of 1.00 equimolar TEA to sample a; (c) after further addition of 1.50 equimolar TFA to sample b.

*11. [1]H NMR experiments of the cyanide-responsiveness of **MCCG***

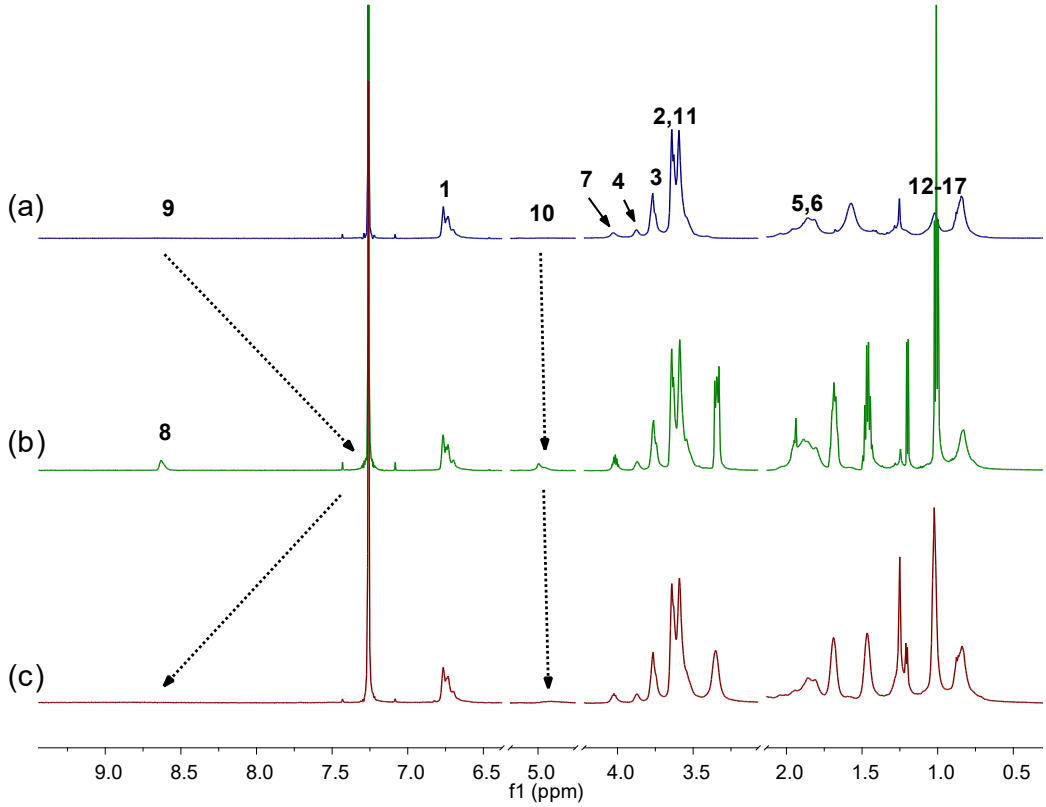

Fig. S20 Partial ^{1}H NMR spectra (600 MHz, $CDCl_3$, 298 K): (a) The gel **MCCG** (5.00 mM); (b) After addition of 0.500 equimolar tetrabutylammonium cyanide to sample a; (c) After further addition of 0.500 equimolar Cu(II) to sample b.

*12. XRD experiments of the cyanide-responsiveness of **MCCG***

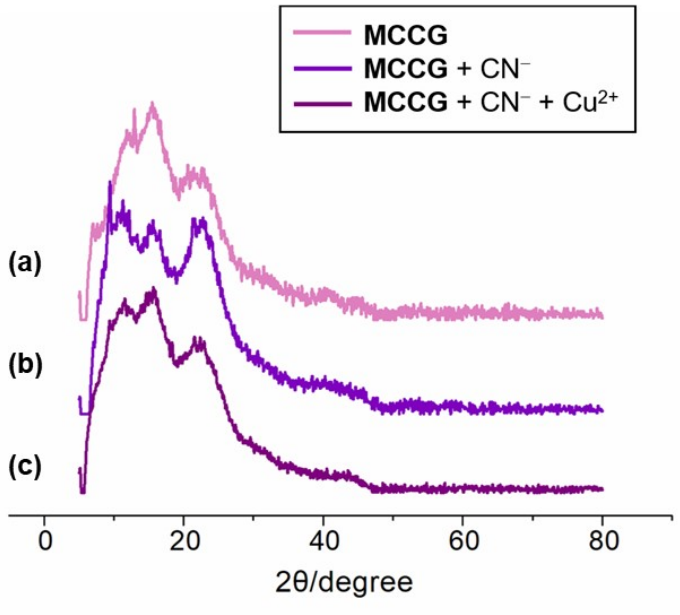

Fig. S21 XRD analysis: (a) **MCCG**; (b) after addition of 0.500 equimolar tetrabutylammonium cyanide to sample a; (c) after further addition of 0.500 equimolar Cu(II) to sample b.

*13. XRD experiments of the conversion of **MCCG** to **HGCG***

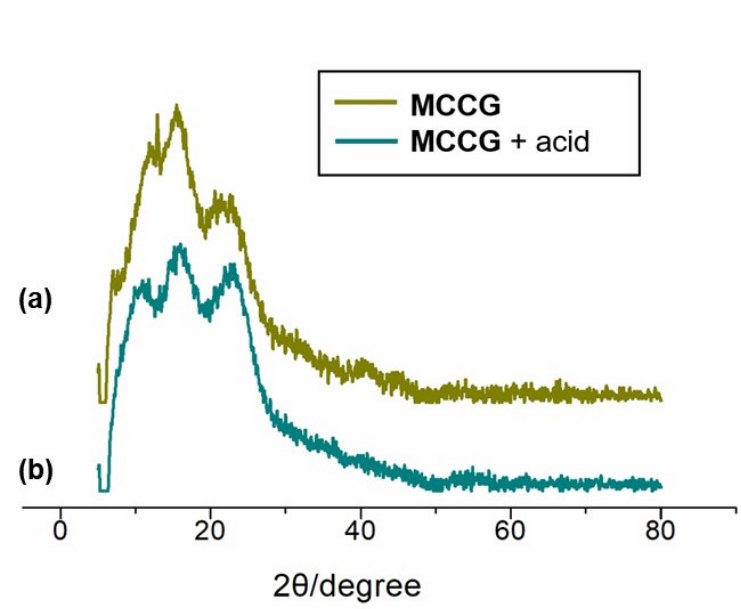

Fig. S22 XRD analysis: (a) **MCCG**; (b) after addition of 1.00 equimolar TFA to sample a.

*14. [1]H NMR experiments of the conversion of **HGCG** to **MCCG***

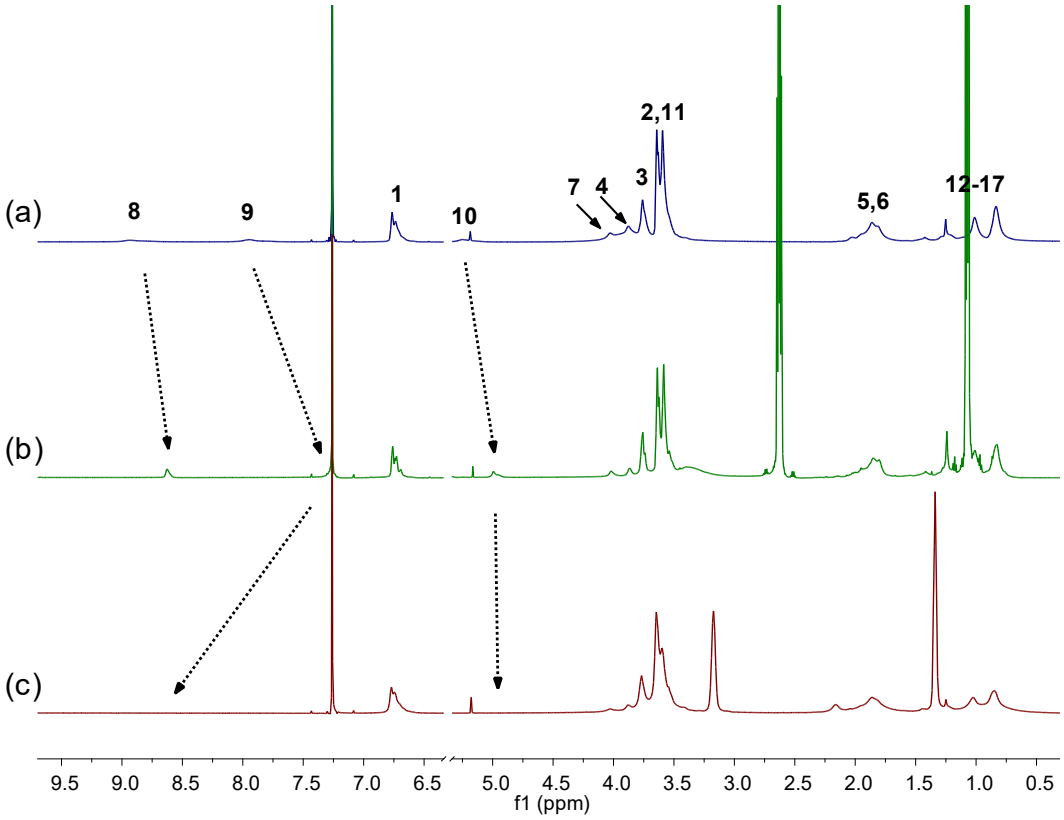

Fig. S23 Partial [1]H NMR spectra (600 MHz, $CDCl_3$, 298 K): (a) The gel **HGCG** (5.00 mM); (b) After addition of 1.00 equimolar TEA to sample a; (c) After further addition of 0.500 equimolar Cu(II) to sample b.

*15. XRD experiments of the conversion of **HGCG** to **MCCG***

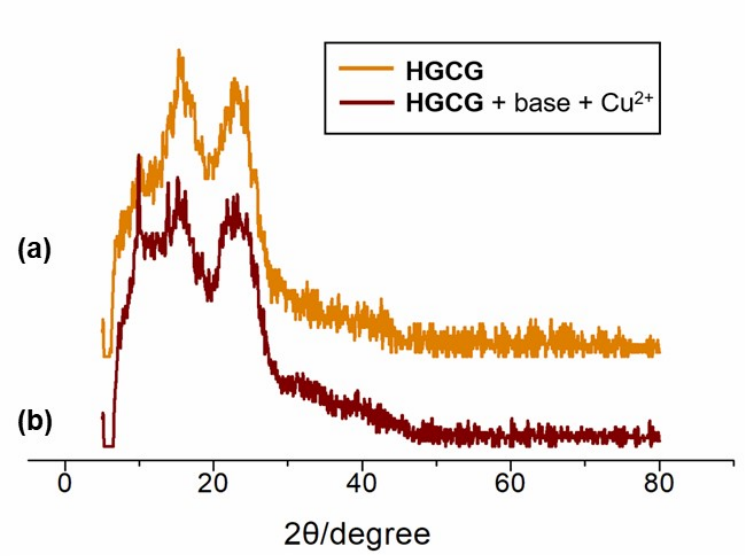

Fig. S24 XRD analysis: (a) **HGCG**; (b) after addition of 1.00 equimolar TEA and 0.500 equimolar Cu(II) to sample a.

*16. ^{1}H NMR experiments of the photo-responsive ability of **P**, **HGCG** and **MCCG***

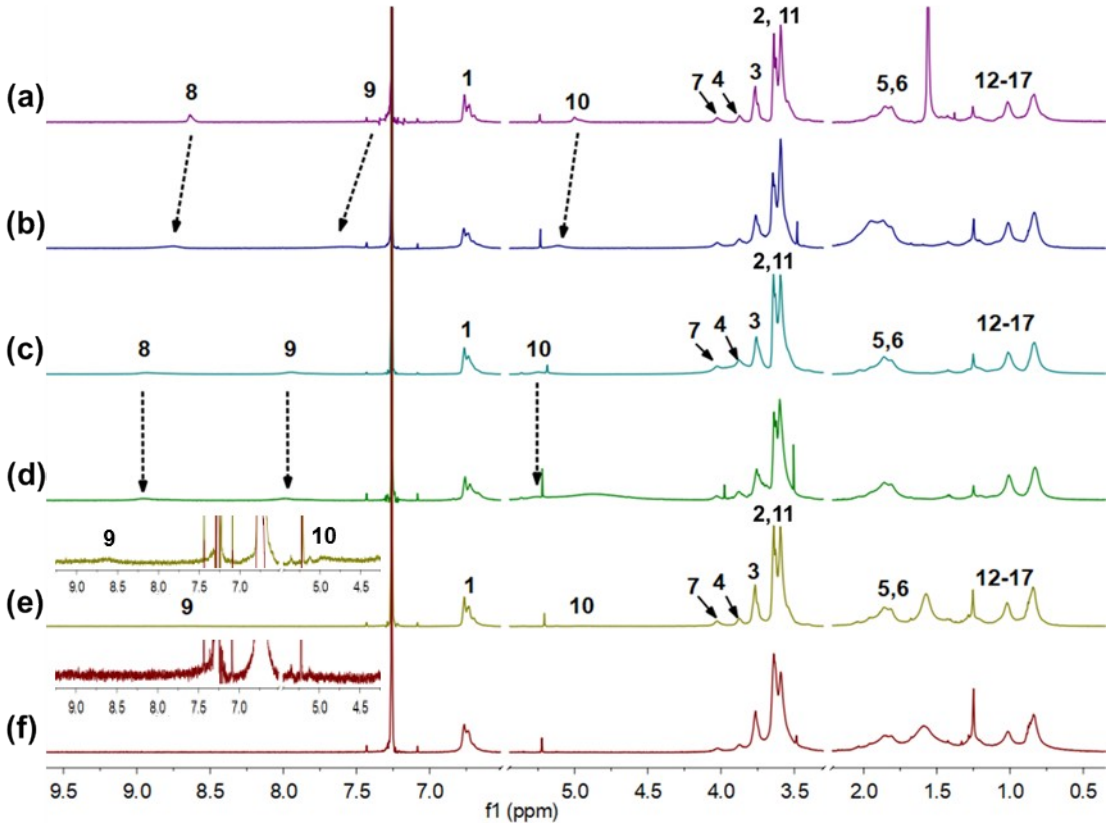

Fig. S25 Partial ^{1}H NMR spectra (600 MHz, $CDCl_3$, 298 K): (a) **P** (5.00 mM); (b) **P** after irradiation at 365 nm for 2 hours; (c) The gel **HGCG** (5.00 mM); (d) The gel **HGCG** after irradiation at 365 nm for 2 hours; (e) The gel **MCCG** (5.00 mM); (f) The gel **MCCG** after irradiation at 365 nm for 2 hours.

*17. FT-IR analysis of the photo-responsive ability of **P**, **HGCG** and **MCCG***

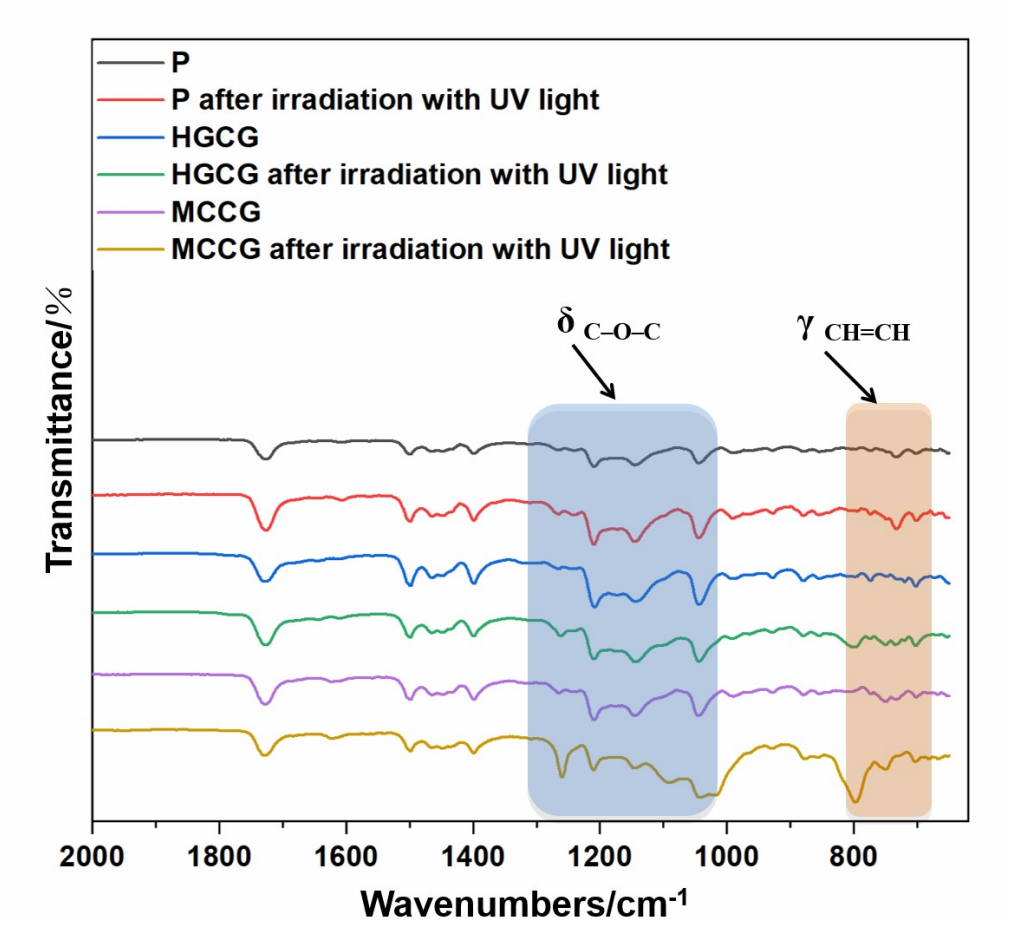

Fig. S26 FT-IR spectra of **P** (black); **P** after irradiation with UV ligh for 8 hours(red); the gel **HGCG** (blue); the gel **HGCG** after irradiation with UV light for 8 hours (green); the gel **MCCG** (purple) and the gel **MCCG** after irradiation with UV light for 8 hours (yellow).

18. SEM images of the gels with multiple stimuli-responsive

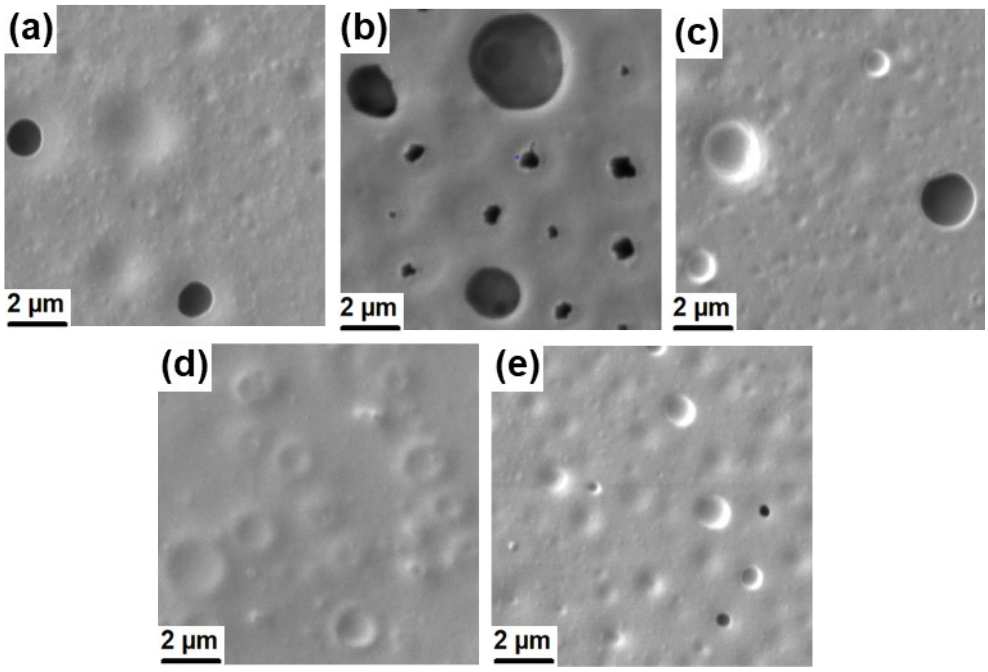

Fig. S27 SEM image: (a) SEM image of the gold-coated of **P** (20.0 mM) after irradiation with UV light at 365 nm for 2 hours in chloroform after drying; (b) SEM image of the gold-coated of the gel **HGCG** (20.0 mM) after addition of 1 equimolar TEA in chloroform after drying; (c) SEM image of the gel **HGCG** (20.0 mM) after irradiation with UV light at 365 nm for 2 hours in chloroform after drying; (d) SEM image of the gold-coated of the gel **MCCG** (20.0 mM) after addition of 1 equimolar tetrabutylammonium cyanide in chloroform after drying; (e) SEM image of the gold-coated of the gel **MCCG** (20.0 mM) after irradiation with UV light at 365 nm for 2 hours in chloroform after drying.

*19. Stress–strain curves of **HGCG** and **MCCG***

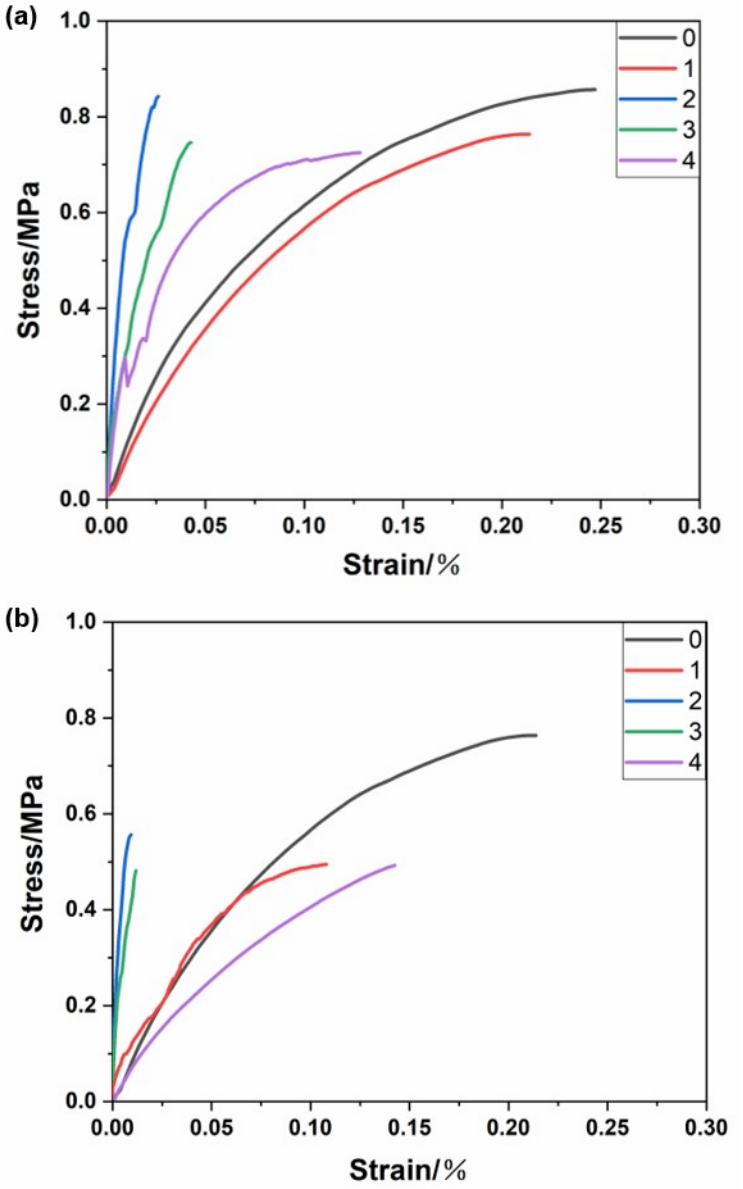

Fig. S28 Stress–strain curves of the gel **HGCG** (a) and the gel **MCCG** (b) of the initial tensile rupture (black line: 0) and the recovery tensile rupture after reattaching for 24 hours of four times consecutive cycle tests (red line: 1; blue line: 2; green line: 3; purple line: 4).

References:

S1. T. Ogoshi, S. Kanai, S. Fujinami, T.-a. Yamagishi and Y. Nakamoto, *J. Am. Chem. Soc.*, 2008, **130**, 5022–5023.

S2. T. Zhou, Y. Lei, H. Zhang, P. Zhang, C. Yan, Z. Zheng, Y. Chen and Y. Yu, *ACS Appl. Mater. Interfaces.*, 2016, **8**, 23431–23436.

S3. X. Yang, W. Cai, S. Dong, K. Zhang, J. Zhang, F. Huang, F. Huang and Y. Cao, *ACS Macro. Lett.*, 2017, **6**, 647–651.

S4. J. Chang, Q. Zhao, L. Kang, H. Li, M. Xie and X. Liao, *Macromolecules*, 2016, **49**, 2814–2820.

S5. H. Ju, C. N. Zhu, H. Wang, Z. A. Page, Z. L. Wu, J. L. Sessler and F. Huang, *Adv. Mater.*, 2022, **34**, 2108163.

S6. P. Wang, X. Yan and F. Huang, *Chem. Commun.*, 2014, **50**, 5017–5019.